LETTERS
PUBLISHED ONLINE: 7 NOVEMBER 2010 | DOI: 10.1038/NGEO1008
nature geoscience

Changes in the sea surface temperature threshold for tropical convection

Nathaniel C. Johnson[1]* and Shang-Ping Xie[2]

Deep convection over tropical oceans is observed generally above a threshold for sea surface temperatures[1–4], which falls in the vicinity of 26–28 °C. High-resolution models suggest that the related sea surface temperature threshold for tropical cyclones rises in a warming climate[5,6]. Some observations for the past few decades, however, show that tropical tropospheric warming has been nearly uniform vertically[7,8], suggesting that the troposphere may have become less stable and casting doubts on the possibility that the sea surface temperature threshold increases substantially with global warming. Here we turn to satellite observations of rainfall for the past 30 years. We detect significant covariability between tropical mean sea surface temperatures and the convective threshold on interannual and longer timescales. In addition, we find a parallel upward trend of approximately 0.1 °C/decade over the past 30 years in both the convective threshold and tropical mean sea surface temperatures. We conclude that, in contrast with some observational indications, the tropical troposphere has warmed in a way that is consistent with moist-adiabatic adjustment, in agreement with global climate model simulations.

The existence of the sea surface temperature (SST) threshold for convection is a well-known phenomenon with important implications for defining the regions of tropical cyclone development[5,6], understanding mechanisms that regulate tropical temperature[4,9,10] and delineating convectively active regions in the tropics. The physical explanation for the SST threshold relates to the strong dependence of atmospheric instability on local SST over the tropical oceans, which owes to two important characteristics of the tropical troposphere: the strong relationship between boundary-layer moist static energy and SST, and the weak horizontal gradients in free-tropospheric temperature. As the relative humidity and air–sea temperature difference exhibit rather limited variability in the tropical oceanic boundary layer, the boundary-layer moist static energy depends largely on SST, with the largest values over the highest SST. In the free troposphere, equatorial waves efficiently smooth out temperature gradients so that tropical free-tropospheric temperatures vary horizontally less than the SST (ref. 11). As a result of these two characteristics, convective instability in the tropics depends largely on the local SST, and the SST threshold for convection corresponds approximately to the minimum SST that can generate finite convective available potential energy (CAPE) through a deep layer of the troposphere[12–14].

As the SST threshold for convection is tied to convective instability, this threshold must be strongly related to the tropical upper-tropospheric temperature. Observations show that tropospheric temperatures in the tropics approximately follow a moist-adiabatic temperature profile, which suggests an adjustment of upper-tropospheric temperatures in response to surface temperatures in the tropics[15]. This hypothesis of moist-adiabatic lapse rate (MALR) adjustment predicts a close covariability between the SST threshold and tropical mean SST. If true, the variability and long-term trend of the SST threshold may reveal important information about the variability and trends in the tropical troposphere. We test this hypothesis with the use of observations spanning multiple decades and with state-of-the-art global climate models. For the observational data, we use two widely used global precipitation products, the Global Precipitation Climatology Project[16] (GPCP) and the Climate Prediction Center merged analysis of precipitation[17] (CMAP), which provide precipitation estimates based on a mix of satellite and rain gauge measurements from 1979 until present. Despite differences in both the tropical mean precipitation rate and long-term trend in these two data sets[18], we examine the possibility that regional changes in precipitation and their relationships to SST, including the SST threshold, may be more detectable than the long-term trend in tropical precipitation.

Figure 1 illustrates the 30-year time series of both the annual mean tropical SST (ref. 19) and two estimates of the SST threshold for convection. In one estimate, we determine the SST threshold

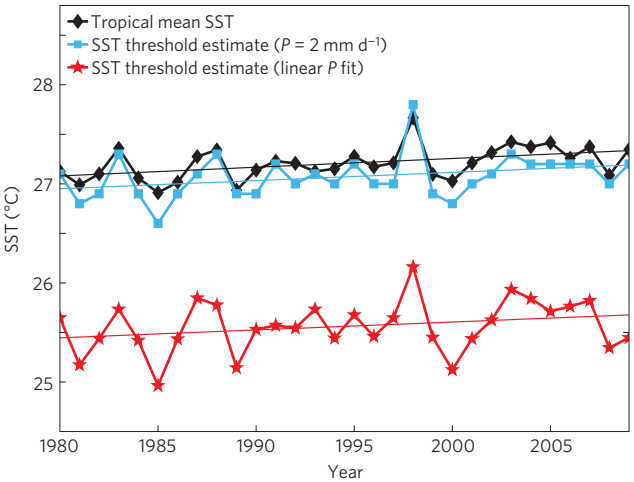

Figure 1 | Time series of tropical mean SST and the SST threshold for convection. Thirty-year time series of annual tropical mean (20° S to 20° N) SST (black diamonds) and two estimates of the SST threshold for convection (blue squares and red stars). Linear trend lines are also shown. The linear trends with 95% confidence intervals for the tropical mean SST, the $P = 2$ mm d^{-1} SST threshold estimate and the linear P fit SST threshold estimate are 0.088 ± 0.057, 0.083 ± 0.076 and 0.080 ± 0.113 °C per decade, respectively. The effective degrees of freedom in the 95% confidence interval calculations account for the lag-1 autocorrelation in the residual time series.

[1]International Pacific Research Center, SOEST, University of Hawaii at Manoa, Honolulu, Hawaii 96822, USA, [2]International Pacific Research Center and Department of Meteorology, SOEST, University of Hawaii at Manoa, Honolulu, Hawaii 96822, USA. *e-mail: natj@hawaii.edu.

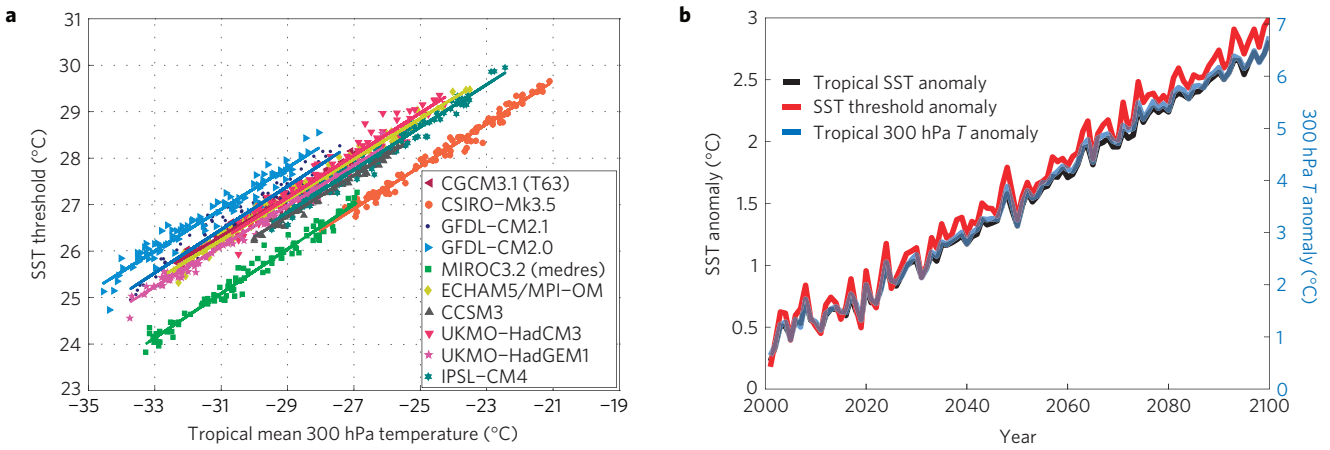

Figure 2 | The relationship between the SST threshold for convection and upper-tropospheric temperature in global climate models. a, Scatter plot of SST threshold versus tropical mean 300 hPa temperature with regression lines for each of ten CMIP3 models under emissions scenario A1B in simulations of the twenty-first century. **b**, Ensemble mean tropical mean SST (black), SST threshold for convection (red) and tropical mean 300 hPa temperature (blue) anomaly time series for the CMIP3 models. Anomalies are relative to the 1961–1990 climatology. The left *y* axis corresponds to the tropical mean SST and SST threshold, whereas the right *y* axis corresponds to the 300 hPa temperature. The scaling for the 300 hPa temperature (right *y* axis) corresponds approximately to that of MALR adjustment of the tropical mean SST (left *y* axis).

by finding the minimum SST for which the mean precipitation rate (P) exceeds 2 mm d^{-1}, and in the other, we approximate P as a linear function of SST above a threshold[20] (see the Methods section). Although the magnitude of the SST threshold depends on the method of determination, the variability does not: both estimates show a remarkable correspondence between the tropical mean SST and the convective threshold ($r \geq 0.88$). In Fig. 1 we present results based on GPCP data, but results based on CMAP data are similar. Both the tropical mean SST and the SST threshold for convection have undergone an upward trend of approximately 0.1 °C per decade (see Supplementary Table S1).

The SST threshold exhibits substantial variability on shorter timescales as well. The range of the detrended annual time series exceeds 1 °C for all estimates, and the standard deviation exceeds 0.2 °C (see Supplementary Table S1), which clearly reflects, in large part, variability associated with the El Niño/Southern Oscillation. Figure 1 indicates that the interannual variability of the SST threshold slightly exceeds that of the tropical mean SST, a characteristic that is reproduced by global climate models (see Supplementary Fig. S3 and the corresponding discussion in the Supplementary Information). The strong coupling with the tropical mean SST on interannual timescales is consistent with the previously reported link between tropical mean and 'rainy region' ($P > 6$ mm d^{-1}) SST (ref. 21).

Next, we examine SST threshold variability in ten global climate models of the Fourth Assessment Report of the Intergovernmental Panel on Climate Change (IPCC AR4), through the use of the World Climate Research Program Coupled Model Intercomparison Project 3 (WCRP CMIP3; ref. 22) multi-model database archive (see Supplementary Table S2 for a list of the ten models used). Despite differences in the simulated tropical climate among the models and consistent with ref. 10, all ten models exhibit a similarly strong correspondence between the tropical mean SST and the SST threshold on all timescales. In all cases but one, the correlation coefficient between the tropical mean SST and SST threshold equals or exceeds 0.90 for the climate of the twentieth century (20C3M) simulations and for the twenty-first-century emissions scenario A1B simulations (see Supplementary Table S2 and Supplementary Fig. S1).

According to our central hypothesis regarding the response of the SST threshold to MALR adjustment, the strong coupling between the SST threshold and tropical mean SST in observations (Fig. 1) and in the CMIP3 models represents an indirect link, with the upper-tropospheric temperature response to the tropical mean SST serving as the intermediary. The testing of this hypothesis with observational data is difficult because of the uncertainty of tropical upper-tropospheric temperature trends in observations. As a result of this limitation, we examine the link between the SST threshold for convection and upper-tropospheric temperature in the CMIP3 models. Figure 2a illustrates scatter plots of SST threshold versus tropical mean 300 hPa temperature in the ten CMIP3 models in simulations of the twenty-first century climate under the A1B scenario. Despite the differences in the simulated tropical mean state, as evidenced by the scatter among the models, there is a remarkable correspondence between the SST threshold and the tropical mean 300 hPa temperature for each individual model. On the basis of the regression of SST threshold on tropical mean 300 hPa temperature, the tropical mean 300 hPa temperature explains, in a statistical sense, more than 92% of the variance of the convective threshold in all of the climate models. In addition, the values of the regression coefficients (0.42–0.48 °C per °C) are consistent with the values that we would expect if the SST threshold were responding to MALR adjustment of the tropical troposphere (~0.43 °C per °C). The reason that some regression coefficients slightly exceed the expected MALR adjustment value relates to the enhanced SST threshold variability on interannual timescales, as discussed in the Supplementary Information, but this difference clearly is small.

Although previous studies have noted the link between tropical mean SST and tropical tropospheric temperature in observations on interannual timescales[21,23], the long-term trend in upper-tropospheric temperature, as mentioned above, has remained a matter of controversy. MALR adjustment entails enhanced warming in the upper troposphere relative to the surface, but the Working Group I Report of the IPCC AR4 points out the discrepancy between theoretical expectations and observed trends, noting that it is uncertain whether tropospheric warming has exceeded that at the surface since 1979 (ref. 24). Indeed, both radiosonde temperature data[8] and at least one satellite-derived data set[7] suggest less warming in the tropical troposphere relative to the surface over the past 30 years, which would mean that the tropical troposphere has become more unstable in recent decades. As long-term trends in these data sets are known to

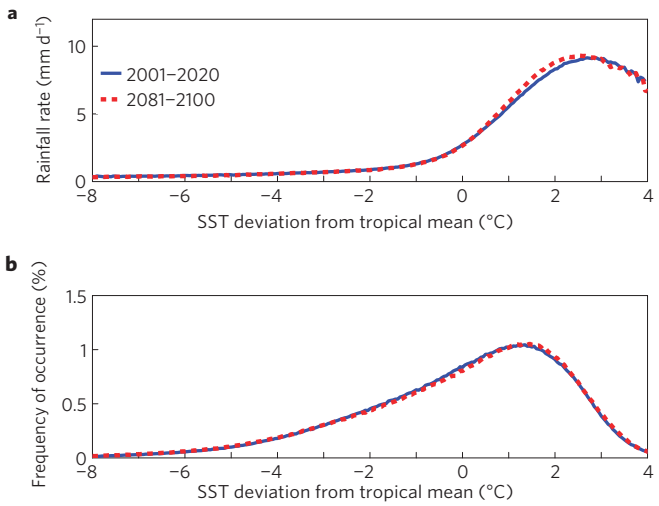

Figure 3 | Twenty-first-century changes in rainfall rate and SST frequency distributions. a,**b**, Ensemble mean rainfall rate as a function of SST (**a**) and SST frequency distribution (**b**) for 2001–2020 (blue, solid) and 2081–2100 (red, dashed) for the ten CMIP3 models of Fig. 2. SST is expressed as the deviation from the 20-year tropical mean.

be affected by non-climatic artefacts, recent attempts to produce better homogenized records[25,26] and to incorporate dynamical information[27] in reconstructing tropospheric temperature trends have yielded upper-tropospheric warming estimates closer to the moist-adiabatic expectation. However, substantial uncertainty still accompanies these revised estimates.

On the basis of the thermodynamic arguments presented above, the similarity between the trends of SST and the SST threshold for convection in Fig. 1 is consistent with approximate MALR adjustment in observations and inconsistent with reduced upper-tropospheric warming relative to the surface, as indicated in some observational data sets. Although the statistical uncertainty of 30-year trends is rather high, the clean relationship between the SST threshold and tropical mean SST at all timescales in both observations and models increases confidence that the tropical atmosphere is warming in a manner that is broadly consistent with theoretical MALR expectations. These results suggest that, in addition to dynamical considerations related to thermal wind adjustment[27], thermodynamic considerations related to the SST threshold for convection may provide important clues for understanding tropical tropospheric changes under global warming.

Figure 2b clearly illustrates the strong link between convective threshold, tropical mean SST and MALR adjustment in the climate models' simulation of the twenty-first-century tropical climate. As a result of the mean state variability among the models, all values in Fig. 2b are expressed as anomalies relative to the 1961–1990 mean. This figure shows that both the tropical mean SST and threshold are projected to increase by approximately 3 °C, relative to the 1961–1990 mean, by the year 2100, with the SST threshold increase consistent with MALR adjustment.

The nearly perfect correspondence between changes in tropical mean SST and SST threshold for convection suggests that the fractional area of the tropical oceans that is convectively active may change little, despite the projection of a substantial increase in boundary-layer moisture in a warmer climate[28,29]. Figure 3 provides evidence of this claim in the CMIP3 climate model simulations. This figure illustrates the ensemble mean rainfall rate as a function of SST (Fig. 3a) and the SST frequency distribution (Fig. 3b), for two 20-year periods, 2001–2020 and 2081–2100, under the A1B scenario. Here, SST is defined as the deviation from the tropical mean for the 20-year period. Figure 3 reveals remarkable similarity in the curves between the two periods, which suggests that, relative to the tropical mean SST, the rainfall rate and SST frequency distributions are projected to change little under global warming. Inspection of the curves for the individual models (Supplementary Fig. S4) reveals differences in the shape of the curves among the models, but all models share this near invariance of the distribution shape with time. This result is consistent both with the SST threshold for convection following the tropical mean SST and with the near invariance of the convectively active fractional area; both characteristics seem to be a consequence, in part, of the nearly constant tropical moist instability owing to MALR adjustment. In observations, we see some evidence of this second characteristic as well, as the area exceeding the 27 °C sea surface isotherm has increased by 3% in 2000–2009 relative to 1980–1989, but the fractional area with rainfall rates exceeding 2 mm d^{-1} has remained nearly constant or has even decreased slightly (see Supplementary Fig. S5 and the corresponding discussion in the Supplementary Information). The implications of Fig. 3 also support the recent claim that local changes in tropical precipitation may follow closely the patterns of sea surface warming, that is, the deviation between the local and the tropical mean SST change, rather than the local SST change alone[30]. On the basis of the results presented here, we add that local changes in SST probably will not significantly impact local precipitation unless the local SST is above the threshold for convection.

The variability of the tropical SST threshold for convection is robust and clearly detectable in both observations and in global climate models. As a result of the inextricable link between the SST threshold and upper-tropospheric conditions, the examination of the SST threshold may provide important information on tropical tropospheric trends under global warming, particularly given the non-climatic artefacts found in radiosonde and satellite-derived data sets. Both the observational data and model simulations indicate that, as a consequence of approximate MALR adjustment, the SST threshold for convection has risen and will continue to rise in tandem with the tropical mean SST.

Methods

Data. For the observational analyses we use monthly mean data of the Extended Reconstructed Sea Surface Temperature (ERSST) Version 3b (ref. 19), GPCP (ref. 16) and CMAP (ref. 17) data sets for the years 1979–2009. We consider the ocean regions of the deep tropics from 20° S to 20° N. For the observational analyses, we also extended the domain (25° S to 25° N and 30° S to 30° N) and obtained qualitatively similar results. As the SST (2° latitude–longitude grid) and precipitation (2.5° latitude–longitude grid) data are located on different grids, we linearly interpolate the ERSST data to the precipitation data grid for the SST threshold for convection calculations, described below.

For the IPCC AR4 model analyses, we use monthly mean SST, precipitation rate and 300 hPa temperature data from ten global climate models (see Supplementary Table S2) from the WCRP CMIP3 (ref. 22) database archive. For each model, we analyse one simulation for the 20C3M and special emissions report A1B scenarios (run 1 for each model except run 2 for the 20C3M simulation of CCSM3). All analyses consider the ocean regions of the deep tropics (20° S to 20° N), except that the tropical mean 300 hPa temperature calculations consider the entire deep tropics.

SST threshold for convection calculations. For each year (September to August) in the analysis, we calculate the mean precipitation rate corresponding to SST binned at intervals of 0.1 °C. We define the year as September to August to maximize the interannual variability associated with the El Niño/Southern Oscillation, as this 12-month interval correlates most strongly with the November–January Niño 3.4 index in observations, but the results presented here are not sensitive to this choice of annual mean.

We calculate the annual SST threshold for convection in two ways. In the first way, we consider tropical ocean rainfall as a linear function of SST above a threshold:

$$P(T_s, t) = b(t)[T_s - T_{s,\mathrm{thresh}}(t)]H[T_s - T_{s,\mathrm{thresh}}(t)] \quad (1)$$

where P is the rainfall rate as a function of SST T_s and year t, $b(t)$ is the slope parameter, $T_{s,\mathrm{thresh}}$ is the SST threshold for convection and H denotes the

Heaviside function. We determine b and $T_{s,thresh}$ for each year through a nonlinear optimization procedure that minimizes the squared error between the actual precipitation rate curve produced by binning, as described above, and the curve approximated by equation (1). As convective instability in the tropics is determined largely by SST, as discussed in the main text, the use of equation (1) is approximately equivalent to the expression of tropical rainfall rate as a linear function of annual mean CAPE. Observations support the strong link between tropical SST and mean CAPE (ref. 20) and the linear relationship between tropical convection and mean CAPE (ref. 13), although we recognize that exceptions to this relationship exist for some locations and time periods[14,20]. To avoid fitting P for infrequently visited SST bins where the precipitation rates are very noisy, we limit the fitting to SSTs less than 2.5 °C above the annual tropical mean SST. This limitation has some theoretical support through considerations of the upper moist convective SST limit[4], and so the highest observed SSTs above this limit are likely to be associated with large-scale conditions that tend to suppress convection.

In the second method of SST threshold calculation, we define an arbitrary rainfall rate limit of 2 mm d^{-1}, and find the minimum SST for which the mean rainfall rate exceeds this value. As a result of noise in the annual rainfall rate curves, we add the condition that the rainfall rate must exceed this limit for at least three consecutive SST bins. We obtain similar results with different rainfall rate limits and with different SST bin persistence criteria. In terms of variability, which is the focus of this study, the results are rather insensitive to the choice of method for estimating the SST threshold for convection.

For the precipitation rate curves of Fig. 3a, we similarly calculate the mean precipitation rate for SST bins, but in this case and for the frequency calculations of Fig. 3b, we use an SST interval of 0.05 °C.

Received 9 August 2010; accepted 11 October 2010; published online 7 November 2010

References

1. Gadgil, S., Joseph, V. & Joshi, N. V. Ocean-atmosphere coupling over monsoon regions. *Nature* **312,** 141–143 (1984).
2. Graham, N. E. & Barnett, T. P. Sea surface temperature, surface wind divergence, and convection over tropical oceans. *Science* **238,** 657–659 (1987).
3. Zhang, C. Large-scale variability of atmospheric deep convection in relation to sea surface temperature in the tropics. *J. Clim.* **6,** 1898–1913 (1993).
4. Sud, Y. C., Walker, G. K. & Lau, K-M. Mechanisms regulating sea-surface temperatures and deep convection in the tropics. *Geophys. Res. Lett.* **26,** 1019–1022 (1999).
5. Yoshimura, J., Sugi, M. & Noda, A. Influence of greenhouse warming on tropical cyclone frequency. *J. Meteorol. Soc. Jpn* **84,** 405–428 (2006).
6. Knutson, T. R., Sirutis, J. J., Garner, S. T., Vecchi, G. A. & Held, I. M. Simulated reduction in Atlantic hurricane frequency under twenty-first-century warming conditions. *Nature Geosci.* **1,** 359–364 (2008).
7. Santer, B. D. *et al*. Amplification of surface temperature trends and variability in the tropical atmosphere. *Science* **309,** 1551–1556 (2005).
8. Karl, T. R., Hassol, S. J., Miller, C. D. & Murray, W. L. (eds) in *Temperature Trends in the Lower Atmosphere: Steps for Understanding and Reconciling Differences* (A report by the Climate Change Science Program and the Subcommittee on Global Change Research, Washington, 2006).
9. Pierrehumbert, R. T. Thermostats, radiator fins, and the local runaway greenhouse. *J. Atmos. Sci.* **52,** 1784–1806 (1995).
10. Williams, I. N., Pierrehumbert, R. T. & Huber, M. Global warming, convective threshold, and false thermostats. *Geophys. Res. Lett.* **36,** L21805 (2009).
11. Sobel, A. H., Nilsson, J. & Polvani, L. M. The weak temperature gradient approximation and balanced tropical moisture waves. *J. Atmos. Sci.* **58,** 3650–3665 (2001).
12. Williams, E. & Renno, N. An analysis of the conditional instability of the tropical atmosphere. *J. Clim.* **121,** 21–36 (1993).
13. Bhat, G. S., Srinivasan, J. & Gadgil, S. Tropical deep convection, convective available potential energy and sea surface temperature. *J. Meteorol. Soc. Jpn* **74,** 155–166 (1996).
14. Fu, R., Del Genio, A. D. & Rossow, W. B. Influence of ocean surface conditions on atmospheric vertical thermodynamic structure and deep convection. *J. Clim.* **7,** 1092–1108 (1994).
15. Stone, P. H. & Carlson, J. H. Atmospheric lapse rate regimes and their parameterization. *J. Atmos. Sci.* **36,** 415–423 (1979).
16. Adler, R. F. *et al*. The Version 2 Global Precipitation Climatology Project (GPCP) monthly precipitation analysis (1979–Present). *J. Hydrometeorol.* **4,** 1147–1167 (2003).
17. Xie, P. & Arkin, P. A. Global precipitation: A 17-year monthly analysis based on gauge observations, satellite estimates, and numerical model outputs. *Bull. Am. Meteorol. Soc.* **78,** 2539–2558 (1997).
18. Lau, K-M. & Wu, H-T. Detecting trends in tropical rainfall characteristics, 1979–2003. *Int. J. Climatol.* **27,** 979–988 (2007).
19. Smith, T. M., Reynolds, R. W., Peterson, T. C. & Lawrimore, J. Improvements to NOAA's historical merged land–ocean surface temperature analysis (1880–2006). *J. Clim.* **21,** 2283–2296 (2008).
20. Back, L. & Bretherton, C. S. A simple model of climatological rainfall and vertical motion patterns over tropical oceans. *J. Clim.* **22,** 6477–6497 (2009).
21. Sobel, A. H., Held, I. M. & Bretherton, C. S. The ENSO signal in tropical tropospheric temperature. *J. Clim.* **15,** 2702–2706 (2002).
22. Meehl, G. A. *et al*. The WCRP CMIP3 multimodel dataset: A new era in climate change research. *Bull. Am. Meteorol. Soc.* **88,** 1383–1394 (2007).
23. Su, H., Neelin, D. & Meyerson, J. E. Sensitivity of tropical tropospheric temperature to sea surface temperature forcing. *J. Clim.* **16,** 1283–1301 (2003).
24. Solomon, S. (ed.) in *Contribution of Working Group I to the Fourth Assessment Report of the Intergovernmental Panel on Climate Change, 2007* (Cambridge Univ. Press, 2007).
25. Sherwood, S. C., Meyer, C. L., Allen, R. J. & Titchner, H. A. *et al.* Robust tropospheric warming revealed by iteratively homogenized radiosonde data. *J. Clim.* **21,** 5336–5350 (2008).
26. Lanzante, J. R. & Free, M. Comparison of radiosonde and GCM temperature trend profiles: Effects of dataset choice and data homogenization. *J. Clim.* **21,** 5417–5435 (2008).
27. Allen, R. J. & Sherwood, S. C. Warming maximum in the tropical upper troposphere deduced from thermal winds. *Nature Geosci.* **1,** 399–403 (2008).
28. Held, I. M. & Soden, B. J. Robust responses of the hydrological cycle to global warming. *J. Clim.* **19,** 5686–5699 (2006).
29. Vecchi, G. A. & Soden, B. J. Global warming and the weakening of the tropical circulation. *J. Clim.* **20,** 4316–4338 (2007).
30. Xie, S-P *et al*. Global warming pattern formation: Sea surface temperature and rainfall. *J. Clim.* **23,** 966–986 (2010).

Acknowledgements

We thank the NOAA/OAR/ESRL PSD, Boulder, Colorado, USA, for the CMAP, GPCP and ERSST Version 3b data, which were provided by their website at http://www.esrl.noaa.gov/psd/. We acknowledge the modelling groups, the Program for Climate Model Diagnosis and Intercomparison (PCMDI) and the WCRP's Working Group on Coupled Modelling (WGCM) for their roles in making available the WCRP CMIP3 multi-model data set. Support of this data set is provided by the Office of Science, US Department of Energy. N.C.J. and S-P.X. were supported by grants from NOAA, NSF, NASA and JAMSTEC.

Author contributions

Both N.C.J. and S-P.X. contributed to the central ideas presented in the paper. N.C.J. carried out the analysis and wrote the paper. S-P.X. offered guidance and contributed to the editing of the paper.

Additional information

The authors declare no competing financial interests. Supplementary information accompanies this paper on www.nature.com/naturegeoscience. Reprints and permissions information is available online at http://npg.nature.com/reprintsandpermissions. Correspondence and requests for materials should be addressed to N.C.J.